2000-01-01

Rotary Honing: a Variant of the Taylor Paint-Scraper Problem

Christopher Hills
Technological University Dublin, chris.hills@dit.ie

H. Moffatt
University of Cambridge

Recommended Citation

Hill, C.P. and Moffat, H.K.: Rotary honing: a variant of the Taylor paint-scraper problem, Journal of Fluid Mechanics, 2000. Vol. 418, pp.119-135. doi.org/10.21427/xvnd-b280

J. Fluid Mech. (2000), *vol.* 418, *pp.* 119–135. Printed in the United Kingdom

Rotary honing: a variant of the Taylor paint-scraper problem

By CHRISTOPHER P. HILLS AND H. K. MOFFATT†

Department of Applied Mathematics and Theoretical Physics, University of Cambridge, Silver Street, Cambridge CB3 9EW, UK

(Received 24 February 1999 and in revised form 29 February 2000)

The three-dimensional flow in a corner of fixed angle α induced by the rotation in its plane of one of the boundaries is considered. A local similarity solution valid in a neighbourhood of the centre of rotation is obtained and the streamlines are shown to be closed curves. The effects of inertia are considered and are shown to be significant in a small neighbourhood of the plane of symmetry of the flow. A simple experiment confirms that the streamlines are indeed nearly closed; their projections on planes normal to the line of intersection of the boundaries are precisely the 'Taylor' streamlines of the well-known 'paint-scraper' problem. Three geometrical variants are considered: (i) when the centre of rotation of the lower plate is offset from the contact line; (ii) when both planes rotate with different angular velocities about a vertical axis and Coriolis effects are retained in the analysis; and (iii) when two vertical planes intersecting at an angle 2β are honed by a rotating conical boundary. The last is described by a similarity solution of the first kind (in the terminology of Barenblatt) which incorporates within its structure a similarity solution of the second kind involving corner eddies of a type familiar in two-dimensional corner flows.

1. Introduction

One of the simplest and best-known similarity solutions of fluid dynamics is that describing flow in a corner between two rigid planes, one of which slides with steady velocity U relative to the other at constant inclination α (figure 1*a*) (Taylor 1960, 1962; see also Batchelor 1967, p. 224). In the terminology of Barenblatt (1996), this is a similarity solution of the first kind, for which the stream function $\psi_T(r,\theta)$ is determined on dimensional grounds in the form

$$\psi_T = U\psi(r,\theta) = Urf(\theta), \tag{1.1}$$

where

$$f(\theta) = \frac{(\alpha^2 - k\theta)\sin\theta - \theta\sin^2\alpha\cos\theta}{\alpha^2 - \sin^2\alpha}, \tag{1.2}$$

with

$$k = \tfrac{1}{2}(2\alpha - \sin 2\alpha) > 0. \tag{1.3}$$

Here, (r,θ) are plane polar coordinates, and the fluid domain is $0 < \theta < \alpha$.

The corresponding pressure (per unit density) in a liquid of kinematic viscosity ν

† Also Isaac Newton Institute for Mathematical Sciences, 20 Clarkson Road, Cambridge CB3 0EH, UK.

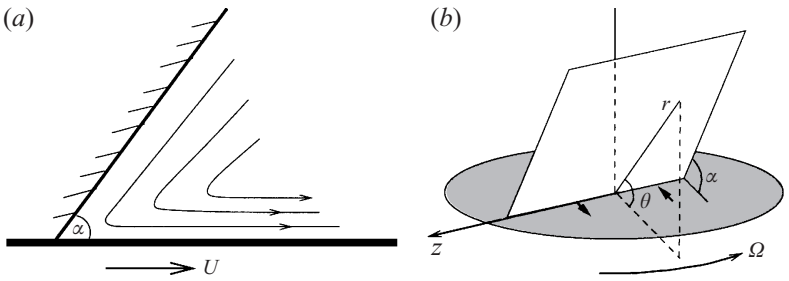

FIGURE 1. (*a*) Two-dimensional geometry of the Taylor paint-scraper problem showing the open streamlines ψ = constant. (*b*) Geometry for the rotary honing problem: a 'blade' is held fixed at angle α above a plate which rotates in its plane with angular velocity Ω.

is given by

$$p_T = p_0 - \nu U g'(\theta)/r, \tag{1.4a}$$

where

$$g(\theta) = f + f'' = -\frac{2(k\cos\theta - \sin^2\alpha\sin\theta)}{\alpha^2 - \sin^2\alpha}, \quad g'(\theta) = \frac{2(k\sin\theta + \sin^2\alpha\cos\theta)}{\alpha^2 - \sin^2\alpha} > 0, \tag{1.4b,c}$$

and p_0 is a positive constant determined by conditions far from the corner. The singularity of pressure at $r = 0$ is a consequence of the imposed discontinuity of velocity at the corner. For $U > 0$, $p_T \to -\infty$ as $r \to 0$, a singularity that would in reality imply cavitation in the immediate vicinity of the corner; for $U < 0$, $p_T \to +\infty$ and an infinite force is required to maintain contact between the planes – in reality, there would in this case be leakage of liquid through a small gap between the planes.

We consider in this paper a variant of this 'scraper' problem, in which the lower plate rotates in its plane with constant angular velocity Ω about a point, taken to be the origin, on the line of intersection of the two planes (figure 1*b*). It is perhaps appropriate to describe this as the 'rotary honing problem', or simply the 'honing problem'. This problem has potential relevance to situations in which viscous fluids are mixed or kept in motion by the rotation of a paddle or rotor, or when fluid is scraped from a smooth surface. Such a situation has been investigated experimentally by Takahashi *et al.* (1982), who consider the mixing of two highly viscous Newtonian fluids by the action of a helical blade in scraping contact with the base of a circular cylinder.

The importance of understanding rotationally driven (mixing) flows has been emphasized by Tatterson, Brodkey & Calabrese (1991), who estimate that the annual cost of solving mixing problems for a typical chemical plant is of the order \$0.5–5 million; and that unaddressed problems could result in a loss of between 0.5% and 3% of the total plant revenue; for the chemical industry in the USA, this amounts to a total potential loss of between \$1–20 billion per annum! This sort of statistic provides ample motivation for the analysis presented in this paper.

We shall find that for the configuration indicated by figure 1(*b*), all three velocity components (u, v, w) are functions of all three cylindrical polar coordinates (r, θ, z), where z is now the 'axial' coordinate parallel to the line of intersection of the planes; even within the Stokes approximation, these velocity components are coupled through the pressure field. The solution in this approximation is determined in §2.

The streamlines of this flow are shown to be the doubly infinite family of closed curves given by the intersections of 'Taylor' surfaces $\psi(r,\theta) = \text{constant}$ and spherical surfaces $r^2+z^2 = \text{constant}$. This is in contrast to the scraper problem of figure 1(*a*), for which all streamlines extend to infinity. However, projection of the closed streamlines of the honing problem on planes $z = \text{constant}$ are segments (doubly covered) of the Taylor curves $\psi = \text{constant}$. This property provides a convenient means for indirect experimental verification of Taylor's solution (see § 4).

The Taylor solution (in the Stokes approximation) is known to be valid in a region where $|U|r/\nu \ll 1$; the Stokes solution for the honing problem may be expected to have a similarly restricted range of validity. By evaluation of the (neglected) inertial terms of the Navier–Stokes equations, we find in § 3 that this neglect is in fact strictly justified only if two conditions are satisfied, namely

$$\Omega r|z|/\nu \ll 1 \quad \text{and} \quad \Omega r^3/|z|\nu \ll 1. \tag{1.5a,b}$$

The second of these conditions means that, no matter how near we are to the origin, there is always a layer near the plane $z = 0$ within which one contribution to these inertial forces (axial convection of momentum) dominates over viscous forces. We adopt an approximation in this layer that takes account of this non-negligible contribution, and compute the resulting inertial perturbation of particle paths. With the inclusion of this effect, the streamlines are no longer exactly closed curves; however the net effect of inertia is still shown to be weak provided merely that the first condition (1.5*a*) is satisfied.

In §§ 5–7, we consider three variants of the honing problem:

(i) The centre of rotation of the lower plane is offset from the line of intersection of the planes; we show in § 5 that to leading order, the particle paths remain closed, the effect of the offset being merely to elongate their shape.

(ii) It is supposed in § 6 that both planes rotate about the same axis through a point on the line of intersection, but with different angular velocities; a frame of reference rotating with the upper plate is chosen, and Coriolis forces are included. These of course do not affect the Stokes solution, but the inertial correction is modified.

(iii) Two vertical plates intersecting at an angle 2β are honed by a conical boundary which rotates about the line of intersection (see figure 10*a* below). A tentative analysis (§ 7) suggests that, in the Stokes approximation, the streamlines again lie on spherical surfaces; moreover on each such surface, a sequence of eddies (cf. Moffatt 1964) may be expected to form near the 2β-corner. This flow is described (again in the terminology of Barenblatt 1996) by a similarity solution of the first kind (one whose structure is determined by dimensional considerations), which contains within this structure a similarity solution of the second kind (one whose crucial scaling parameter is determined by solution of an eigenvalue problem).

2. The Stokes solution to the honing problem

2.1. *Velocity and pressure fields*

With the geometry and coordinate system indicated in figure 1(*b*), the flow in the region $0 < \theta < \alpha$ is given in the Stokes approximation by the equations

$$\nu\nabla^2\boldsymbol{u} = \nabla p, \qquad \nabla\cdot\boldsymbol{u} = 0, \tag{2.1a,b}$$

where $\boldsymbol{u} = (u, v, w)$ is the velocity field relative to the coordinates (r, θ, z), and p is the pressure (per unit density). The boundary conditions are

$$\boldsymbol{u} = 0 \quad \text{on } \theta = \alpha, \quad \text{and} \quad \boldsymbol{u} = (\Omega z, 0, -\Omega r) \quad \text{on } \theta = 0. \tag{2.2a,b}$$

We shall refer to the fixed plane $\theta = \alpha$ as the 'blade', and to the rotating plane as the 'plate' or 'base'.

The first two components of (2.1a) suggest that we try a solution derived from the Taylor solution (1.1), with U simply replaced by Ωz. Thus let

$$\Psi(r, \theta, z) = \Omega z \psi(r, \theta) \quad \text{with still} \quad \psi = r f(\theta), \tag{2.3a,b}$$

and let

$$u = \frac{1}{r}\frac{\partial \Psi}{\partial \theta} = \Omega z f'(\theta), \qquad v = -\frac{\partial \Psi}{\partial r} = -\Omega z f(\theta). \tag{2.4a,b}$$

Here $f(\theta)$ is precisely as given by (1.2); and the first two components of (2.1a) are satisfied provided (cf. (1.4a))

$$p = p_0 - \nu \Omega z g'(\theta)/r, \tag{2.5}$$

where $g(\theta)$ is given by (1.4b).

Consider now the third component of (2.1a):

$$\nu \nabla^2 w = \frac{\partial p}{\partial z} = -\nu \Omega g'(\theta)/r, \tag{2.6}$$

which must be solved with boundary conditions

$$w = 0 \quad \text{on } \theta = \alpha, \qquad w = -\Omega r \quad \text{on } \theta = 0. \tag{2.7a,b}$$

It is very easily verified that the required solution is

$$w = -\Omega r f'(\theta), \tag{2.8}$$

and we note that the boundary conditions (2.2) are satisfied, since by the original construction of Taylor's solution,

$$f(0) = 0, \quad f'(0) = 1, \quad f(\alpha) = f'(\alpha) = 0. \tag{2.9a–d}$$

The solution of (2.1), (2.2) is therefore given by (2.4), (2.5) and (2.8), together with (1.2) and (1.4b, c).

2.2. *Particle paths*

The particle paths of the flow (2.4), (2.8) coincide with the streamlines and are the integral curves of the system $\mathrm{d}r/u = r\,\mathrm{d}\theta/v = \mathrm{d}z/w\,(= \mathrm{d}t)$, i.e.

$$\frac{\mathrm{d}r}{\Omega z f'(\theta)} = \frac{-r\,\mathrm{d}\theta}{\Omega z f(\theta)} = \frac{-\mathrm{d}z}{\Omega r f'(\theta)} = \mathrm{d}t. \tag{2.10}$$

The first equality yields

$$\psi(r, \theta) = r f(\theta) = \text{constant}. \tag{2.11}$$

We may describe these surfaces as the 'Taylor surfaces', since each such surface is obtained by 'sweeping' a Taylor streamline curve in the z-direction. Equality of the first and third terms of (2.10) gives

$$r^2 + z^2 = \text{constant}, \tag{2.12}$$

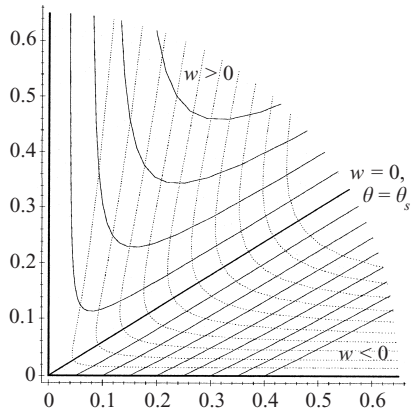

FIGURE 2. Contours $\psi =$ constant (dotted) and $w =$ constant (solid) for the rotary honing problem when the fixed blade $\theta = \pi/2$ is perpendicular to the rotating plate. Note that $w \lessgtr 0$ according as $\theta \lessgtr \theta_s$.

a family of spheres centred on the origin. Thus the particle paths are indeed closed curves, the intersections of these spheres with the Taylor surfaces. This closed-streamline property is to be contrasted with the open-streamline property of the Taylor paint-scraper problem; it is a property that can be tested experimentally (see § 4 below).

The case $\alpha = \pi/2$, for which

$$f(\theta) = \frac{\pi(\pi - 2\theta)\sin\theta - 4\theta\cos\theta}{\pi^2 - 4}, \quad f'(\theta) = \frac{(\pi^2 - 2\pi\theta - 4)\cos\theta - 2(\pi - 2\theta)\sin\theta}{\pi^2 - 4}, \tag{2.13a,b}$$

is of particular interest. Figure 2 shows the contours $\psi = rf(\theta) =$ constant and $w = -\Omega r f'(\theta) =$ constant for this case, and figure 3(*a*) shows a typical streamline as an intersection of a sphere $r^2 + z^2 =$ constant and a Taylor surface $\psi(r, \theta) =$ constant. Note that $f'(\theta) = 0$ when $\theta = \theta_s \approx 30.97^\circ$ and that w changes sign across the line $\theta = \theta_s$. We can picture the motion of a fluid particle as the vector sum of flow along a Taylor curve $\psi =$ constant (which changes direction when the particle crosses the plane $z = 0$) and flow in the z-direction (which changes direction when the particle crosses the plane $\theta = \theta_s$); it is this behaviour that makes the closure of streamlines understandable. Note further that $u = \Omega z f'(\theta)$ is also zero on $\theta = \theta_s$, and the velocity is therefore in the θ-direction on $\theta = \theta_s$ as evident in figure 2; in fact a fluid particle is at its nearest to the origin as it crosses $\theta = \theta_s$. Since $v = 0$ on $z = 0$, the line $z = 0$, $\theta = \theta_s$ is a line of stagnation points of the flow.

Note finally a scaling property of the particle paths obtained from (2.10): if a streamline solution of (2.10) is given in parametric form by $(r(t), \theta(t), z(t))$, then $(\kappa r(t), \theta(t), \kappa z(t))$ is also a solution for arbitrary $\kappa > 0$. Thus the streamlines on a sphere of radius R are geometrically similar (with scale factor κ) to the streamlines on the sphere of radius κR; moreover the orbit time for such geometrically similar streamlines is independent of κ. A set of geometrically similar streamlines (for $\kappa = 1, 2, 3$) is shown for the case $\alpha = \pi/2$ in figure 3(*b*); the set for continuous variation of κ lie on a cone with vertex at the origin.

For general α, the value of θ where $u = w = 0$ is given from solution of the equation

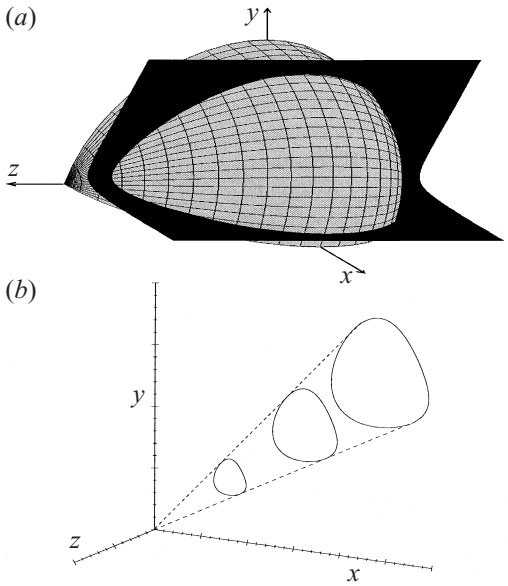

FIGURE 3. (*a*) Flow streamline shown as an intersection of a Taylor surface ψ = constant (black) and a sphere $r^2 + z^2$ = constant (grey) ($x = r\cos\theta$, $y = r\sin\theta$). (*b*) Set of self-similar streamlines for which $\theta = \pi/8$ when $z = 0$, on spheres of radius R, $2R$, $3R$ where R is arbitrary.

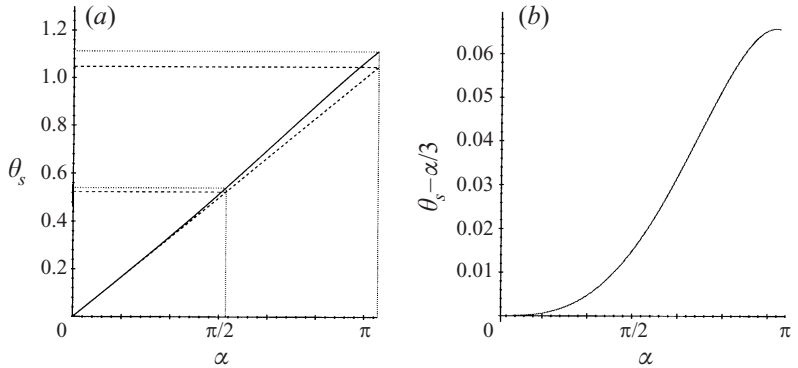

FIGURE 4. (*a*) The angle θ_s of the plane on which $u = w = 0$ as a function of α; the linear approximation $\theta_s \approx \alpha/3$ is shown by the dashed line. (*b*) Expanded view of the difference $\theta_s - \alpha/3$ as a function of α.

$f'(\theta) = 0$, i.e. from (1.2):

$$\tan\theta = \frac{\alpha^2 - \sin^2\alpha - k\theta}{k - \theta\sin^2\alpha}. \tag{2.14}$$

The solution of this transcendental equation, $\theta = \theta_s(\alpha)$, is shown in figure 4; the function $\theta_s(\alpha)$ is asymptotically $\alpha/3$ as $\alpha \to 0$, and is in fact remarkably close to $\alpha/3$ over the whole range $0 < \alpha < \pi$.

2.3. *Force and couple on the scraper*

As already observed in § 1, the r^{-1} singularity in the pressure field associated with the Taylor flow (equation (1.4*a*)) means that this flow cannot be exactly realized in

practice: the singularity must be resolved either geometrically (through a small gap between the plates) or physically (through cavitation or other mechanism).

Consider now the situation for the rotary honing problem. The traction (force per unit area and per unit density) acting on the fixed blade $\theta = \alpha$ is, relative to (r, θ, z) coordinates,

$$\boldsymbol{t} = \left(-\frac{v}{r}\frac{\partial u}{\partial \theta},\ p, -\frac{v}{r}\frac{\partial w}{\partial \theta} \right)_{\theta=\alpha} = v\Omega \left(-\frac{z}{r} f''(\alpha),\ -\frac{z}{r} g'(\alpha),\ f''(\alpha) \right), \tag{2.15}$$

using (2.4), (2.5) and (2.8). Here the contribution due to the constant additional pressure p_0 is ignored. From (1.2) and (1.4*c*), we find

$$f''(\alpha) = \frac{2(\sin\alpha - \alpha\cos\alpha)}{\alpha^2 - \sin^2\alpha}, \qquad g'(\alpha) = \frac{2\alpha\sin\alpha}{\alpha^2 - \sin^2\alpha}. \tag{2.16a,b}$$

The singularity in the r and θ components of stress is still evident in (2.15), so that the same caveat is needed here concerning real-fluid effects in the immediate vicinity of $r = 0$. However, insofar as these components are odd functions of z, they integrate to zero over any even interval $(-z_0, z_0)$. The z-component of stress in (2.15) is independent of r and z, and integrates to give a total force on the blade

$$\boldsymbol{F} = (0, 0, v\Omega A f''(\alpha)), \tag{2.17}$$

where A is the area of the blade, assumed finite in any practical situation.

The moment of the traction $\boldsymbol{t}$ about the origin is

$$\boldsymbol{x} \wedge \boldsymbol{t}\big|_{\theta=\alpha} = \left(\frac{z^2}{r} g'(\alpha), -\frac{(z^2 + r^2)}{r} f''(\alpha), -z g'(\alpha) \right). \tag{2.18}$$

Here the first two components have a non-integrable singularity at $r = 0$. This singularity must again evidently be resolved either geometrically or physically as indicated above. This has a bearing on experimental realization of the flow, as discussed in § 4 below.

3. Inertial effects

3.1. *Estimate of inertia terms*

Let us now estimate the order-of-magnitude of the (so-far-neglected) inertial acceleration $(\boldsymbol{u} \cdot \nabla)\boldsymbol{u}$. It is convenient to decompose this into two parts:

$$(\boldsymbol{u} \cdot \nabla)\boldsymbol{u} = (\tilde{\boldsymbol{u}} \cdot \nabla)\boldsymbol{u} + w\partial \boldsymbol{u}/\partial z, \tag{3.1}$$

where $\tilde{\boldsymbol{u}} = (u, v, 0)$. Then from (2.4) and (2.8) we may easily evaluate

$$(\tilde{\boldsymbol{u}} \cdot \nabla)\boldsymbol{u} = \Omega^2 \left(-\frac{z^2}{r}(f f'' + f^2), 0, z(f f'' - f'^2) \right) \tag{3.2}$$

and

$$w\partial \boldsymbol{u}/\partial z = \Omega^2(-r f'^2, r f f', 0). \tag{3.3}$$

Now compare these expressions with the viscous term

$$v\nabla^2 \boldsymbol{u} = v\Omega \left(\frac{z}{r^2} g', \frac{z}{r^2} g, -\frac{1}{r} g' \right) \tag{3.4}$$

(with $g = f + f''$ as before). Since for any fixed θ, f and its derivatives are $O(1)$ with respect to variation of r and z, it is evident that the two components of $(\tilde{\boldsymbol{u}} \cdot \nabla)\boldsymbol{u}$ are

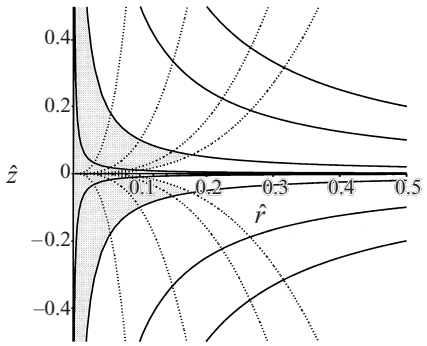

FIGURE 5. Curves $\hat{r}\hat{z} = \text{constant}$ (solid) and $\hat{r}^3/\hat{z} = \text{constant}$ (dotted). Inertia is negligible in the shaded region where $\hat{r}\hat{z} \ll 1$ and $\hat{r}^3/\hat{z} \ll 1$.

negligible compared to the corresponding components of $\nu\nabla^2\boldsymbol{u}$ provided

$$\Omega r|z|/\nu \ll 1. \tag{3.5}$$

We may adopt $Re = \Omega r|z|/\nu$ as a local Reynolds number of the flow, and neglect of inertia certainly requires that $Re \ll 1$.

This however is not sufficient, for comparison of the components of (3.3) with the corresponding components of (3.4) indicates that the inertial contribution $w\partial\boldsymbol{u}/\partial z$ is negligible only if

$$\Omega r^3/\nu|z| \ll 1, \tag{3.6}$$

a condition independent of (3.5). The situation is indicated schematically in figure 5 in which we adopt dimensionless variables $\hat{r} = r(\Omega/\nu)^{1/2}$, $\hat{z} = z(\Omega/\nu)^{1/2}$. It is evident that, no matter how near to the origin we are, the term $w\partial\boldsymbol{u}/\partial z$, representing transport of momentum by the axial component of velocity w, remains important in a neighbourhood of the plane $z = 0$, on which, for reasons of symmetry, the r and θ components of $\nu\nabla^2\boldsymbol{u}$ both vanish.

3.2. *Oseen-type approximation in the inertial layer*

Let us then place ourselves in the region where $Re \ll 1$, but retain the term $w\partial\boldsymbol{u}/\partial z$ in the Navier–Stokes equations; thus we consider the approximation

$$w\partial\boldsymbol{u}/\partial z = -\nabla p + \nu\nabla^2\boldsymbol{u}, \quad \nabla\cdot\boldsymbol{u} = 0, \tag{3.7a,b}$$

where w is as given by the foregoing Stokes analysis, i.e.

$$w = -\Omega r f'(\theta). \tag{3.8}$$

Thus, we continue to neglect inertial terms of relative magnitude $O(\Omega rz/\nu)$, but we retain those of relative magnitude $O(\Omega r^3/z\nu)$. (This partial incorporation of inertial effects is reminiscent of the Oseen approximation for unbounded Stokes flows, and it therefore seems appropriate to describe it as an 'Oseen-type' approximation in the present context also.) We may then expect corresponding perturbations of u, v and p in the form

$$u = \Omega z f' + \Omega^2 r^3 f_2(\theta)/\nu, \qquad v = -\Omega z f + \Omega^2 r^3 g_2(\theta)/\nu, \tag{3.9a,b}$$

$$p = p_0 - \nu\Omega z g'/r + \Omega^2 r^2 p_2(\theta), \tag{3.9c}$$

where f_2, g_2 and p_2 are dimensionless functions of θ to be determined. Note that for $r^3\Omega/v|z| \ll 1$, the leading-order terms in (3.9) dominate and conform to the Stokes solution previously determined.

The additional velocity field in (3.9*a*, *b*) is

$$\boldsymbol{u}_2 = (\Omega^2/v)(r^3 f_2, r^3 g_2, 0) \tag{3.10}$$

and is two-dimensional. The condition $\nabla\cdot\boldsymbol{u}_2 = 0$ implies that $4f_2+g_2' = 0$. Equivalently, $\boldsymbol{u}_2$ is derivable from a streamfunction

$$\psi_2(r,\theta) = -(\Omega^2/4v)r^4 g_2(\theta), \tag{3.11}$$

and the corresponding vorticity is

$$\boldsymbol{\omega}_2 = (\Omega^2/4v)(0,0,r^2 G(\theta)), \tag{3.12}$$

where

$$G = g_2'' + 16g_2. \tag{3.13}$$

Equation (3.7*a*) gives

$$f'^2 = 2p_2 + \tfrac{1}{4}G' \quad \text{and} \quad -ff' = p_2' - \tfrac{1}{2}G, \tag{3.14a, b}$$

and eliminating p_2, we then have

$$G'' + 4G = 8f'(f'' + f) = 8f'g. \tag{3.15}$$

Equations (3.13), (3.15) constitute a fourth-order linear system, and the boundary conditions, deriving from $\boldsymbol{u}_2 = 0$ on $\theta = 0, \alpha$ are

$$g_2 = g_2' = 0 \quad \text{on } \theta = 0, \alpha. \tag{3.16}$$

The term $8f'g$ in (3.15) is a forcing term of known form. The required solution has the form

$$\begin{aligned} g_2(\theta) = [(A_1 + A_2\theta) + (A_3 + A_4\theta)\theta\cos 2\theta + (A_5 + A_6\theta)\theta\sin 2\theta \\ + C_1\cos 2\theta + C_2\sin 2\theta + C_3\cos 4\theta + C_4\sin 4\theta](\alpha^2 - \sin^2\alpha)^{-2}. \end{aligned} \tag{3.17}$$

The constants $A_1, \ldots, A_6$ are determined by satisfying (3.13), (3.15) and the constants $C_1, \ldots, C_4$ are then determined by satisfying the boundary conditions (3.16).

For the particular case $\alpha = \pi/2$, these constants have (with an obvious notation) the following values:

$$(A_i) = \left(-\frac{\pi^3}{64}, \frac{4+\pi^2}{32}, \frac{52-25\pi^2}{288}, \frac{\pi}{12}, \frac{\pi(26-3\pi^2)}{144}, \frac{\pi^2-4}{48}\right) \tag{3.18}$$

and

$$(C_i) = \left(\frac{\pi(11\pi^2-8)}{576}, \frac{(\pi^2+4)(3\pi^2-26)}{1152}, \frac{\pi(4-\pi^2)}{288}, -\frac{(3\pi^4-46\pi^2+72)}{2304}\right). \tag{3.19}$$

It is important to note that (3.8) and (3.9) now provide an exact solution of (3.7) satisfying the boundary conditions (2.2), and that this solution is now uniformly valid in the region where (1.5*a*) is satisfied.

3.3. *Inertial perturbation of particle paths*

The particle paths associated with the velocity field (u, v, w) in (3.8), (3.9) have been computed for the case $\alpha = \pi/2$ and for various initial conditions. Figure 6(*a*) shows

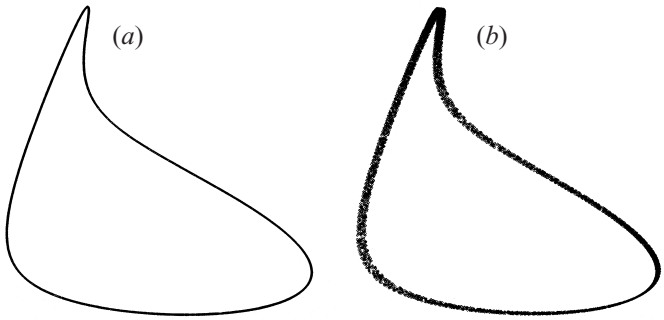

FIGURE 6. Particle path for $\alpha = \pi/2$, with initial position $\hat{r} = 0.05$, $\theta = 0.2$, $\hat{z} = 0$: (*a*) Stokes solution, (*b*) solution incorporating inertial term $w\partial \boldsymbol{u}/\partial z$. In both cases, the time of integration is such that the particle crosses the plane $\hat{z} = 0$ one thousand times.

one such particle path for the Stokes flow determined in § 2, which is as expected a closed curve. Figure 6(*b*) shows the particle path with the same initial conditions and including the additional (inertial) contributions of (3.7*a*, *b*). Both diagrams show a path which crosses the plane $z = 0$ one thousand times. Figure 6(*b*) indicates a slow 'drift' associated with the inertial perturbation experienced on each orbit as the particle crosses the layer in which $z = O(r^3\Omega/\nu)$. Poincaré sections of such paths on the plane $z = 0$ indicate that the drift may be towards or away from the origin, depending on the initial conditions.

The magnitude of this drift may be estimated as follows. On a single orbit, the particle remains very near to a sphere of radius R and the time taken for it to cross the inertial layer of thickness $O(\Omega R^3/\nu)$ with velocity $w \sim \Omega R$ is of order R^2/ν. During this time the net displacement associated with the velocity $\boldsymbol{u}_2$ ($\sim \Omega^2 R^3/\nu$) is of order $\Omega^2 R^5/\nu^2$. Hence the percentage drift in the (r, θ)-plane relative to the scale $O(R)$ of the orbit is given by $100(R/L)^4\%$, where $L = (\nu/\Omega)^{1/2}$. With the specific conditions of figure 6(*b*), $R/L = 0.05$, and for one thousand orbits, this percentage drift amounts to 0.6%, in order-of-magnitude agreement with the computed drift.

Over a long period of time, the cumulative effect of this drift may be to move the particle out of the region of validity $r|z| \ll \nu/\Omega$ of the solution. We should note moreover that the weak $O(Re)$ inertial effect that is neglected in the above treatment provides an additional perturbation over the whole orbit, which may contribute significantly to the net drift in practice.

3.4. *The influence of eddy solutions*

The streamfunction $\psi_2(r, \theta)$ given by (3.11) is a particular solution of the forced biharmonic equation

$$\nabla^4 \psi = -2(\Omega^2/\nu) f' g \tag{3.20}$$

with boundary conditions

$$\psi_2 = \partial \psi_2/\partial \theta = 0 \quad \text{on} \quad \theta = 0, \alpha. \tag{3.21}$$

To this solution, we may add the general solution of the associated homogeneous problem (i.e. the 'complementary function'),

$$\psi_c(r, \theta) = \sum_{n=1}^{\infty} \mathscr{A}_n r^{\lambda_n} f_n(\theta) \tag{3.22}$$

(Moffatt 1964). Here, the λ_n (functions of α) are complex solutions of an eigenvalue problem, and may be ordered so that $1 < \mathbb{R}\lambda_1 < \mathbb{R}\lambda_2 < \ldots$. The functions $f_n(\theta)$ are complex eigenfunctions and the coefficients $\mathscr{A}_n$ in (3.22) are determined (in principle) by conditions far from the corner. The real part of the series (3.22) is understood. We note that more general z-dependent eigenfunctions have the same asymptotic r-dependence as $r \to 0$ (Moffatt & Mak 1999).

The r and θ components of the full flow for $Re \ll 1$ should thus be obtained from a streamfunction

$$\Psi = \Omega z r f(\theta) - \Omega^2 r^4 g_2(\theta)/4\nu + \psi_c(r, \theta). \tag{3.23}$$

We have seen that the second term here dominates the first where $|z| \ll \Omega r^3/\nu$. However, for angles α for which $\mathbb{R}\lambda_1 < 4$, the leading-order 'eddy' contribution in ψ_c will dominate the r^4 contribution in (3.23) and will also dominate the leading term in a region $|z| \sim |\mathscr{A}_1|\Omega^{-1} r^{\mathbb{R}\lambda_1 - 1}$. The condition $\mathbb{R}\lambda_1 < 4$ is in fact satisfied for $\alpha > 81.87°$. In particular, for $\alpha = \pi/2$, $\lambda_1 \approx 3.74 + 1.12\mathrm{i}$, so that the (r, θ) components of the flow are dominated by eddy contributions in a region $|z| \sim |\mathscr{A}_1|\Omega^{-1} r^{2.74}$.

The general question of dominance of inhomogeneous or homogeneous contributions to low-Reynolds-number solutions, and the associated breakdown of local similarity solutions, have been discussed by Moffatt (1979) and Moffatt & Duffy (1980). The situation considered above may be contrasted with the two-dimensional Taylor problem, in which case, as shown by Hancock, Lewis & Moffatt (1981), the eddy contributions are dominated not only by the leading-order (Taylor) solution, but also by the first-order inertial correction.

4. Experimental visualization of the flow

A simple experiment was designed in order to visualize the flow described above, for the case $\alpha = \pi/2$. The apparatus is shown in figure 7(*a*). A Perspex cylinder of height 24 cm and radius 10 cm was centrally placed on a rotating table. A static vertical aluminium blade of width 15 cm and height 21 cm was symmetrically and rigidly fixed very close to the smooth cylinder base, the line of 'contact' passing through the centre of rotation; in practice, a gap of the order of 0.1 mm was always present between the blade and the base. The cylinder was filled with a viscous fluid, pricerine, with dynamic viscosity $15\,\mathrm{g\,cm^{-1}\,s^{-1}}$ and density $1.26\,\mathrm{g\,cm^{-3}}$ (Weast 1971). The angular speed Ω of the table, and so of the cylinder, could be varied over the range 0–$10\,\mathrm{rad\,s^{-1}}$; taking $R = 5\,\mathrm{cm}$, the corresponding range of Reynolds number $\Omega R^2/\nu$ is 0–21. The flow structure was found to be fairly insensitive to Reynolds number in this range. The observations described below were obtained at the value $\Omega = 0.25\,\mathrm{rad\,s^{-1}}$ (i.e. $Re \approx 0.5$).

At this low Reynolds number, inertia effects may be expected to be negligible, and the flow near to the centre of rotation should be reasonably well described by the Stokes solution of § 2 above. Three properties of this Stokes solution can be tested:

(i) the closed-streamline property, and the fact that the projection of these streamlines on vertical planes perpendicular to the blade should follow the Taylor curves $rf(\theta) = \text{constant}$;

(ii) the invariance of the flow (2.4), (2.8) under the symmetry transformation $(r, \theta, z) \to (r, \theta, -z)$, $(u, v, w) \to (-u, -v, w)$, which implies symmetry of the streamlines about the plane $z = 0$;

(iii) the linear relation between $\boldsymbol{u}$ and Ω, and the implied reversibility of the flow under reversal of Ω ($\Omega \to -\Omega$).

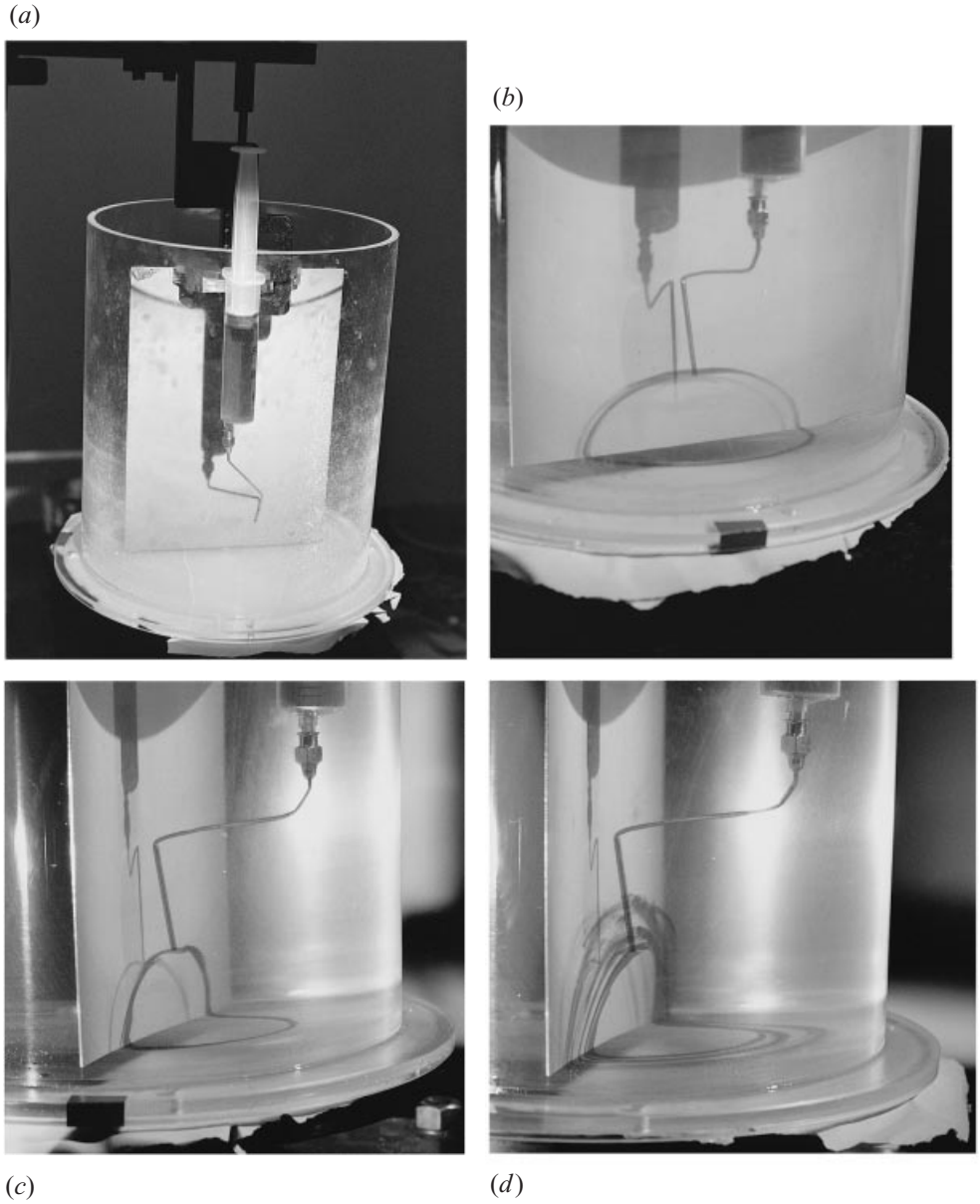

FIGURE 7. (*a*) Experimental apparatus. (*b*) Dye track showing a closed streamline viewed nearly perpendicular to the fixed blade. (*c*) Dye track viewed nearly along the line of intersection of the plates. (*d*) Several adjacent closed streamlines, obtained by moving the point of injection of the dye.

These properties do not persist when inertial effects are included. They may also of course be affected by the 'remote' boundary conditions on the curved surface of the cylinder and at the vertical edges of the blade, and by the presence of the small gap between the blade and the base which allows some leakage of fluid under the blade.

Two visualization techniques were employed. The first used dye, mixed with pricerine to minimize the density difference and injected by hypodermic needle at a point near the fixed blade. Figure 7(*b–d*) shows the resulting dye tracks; these indicate that

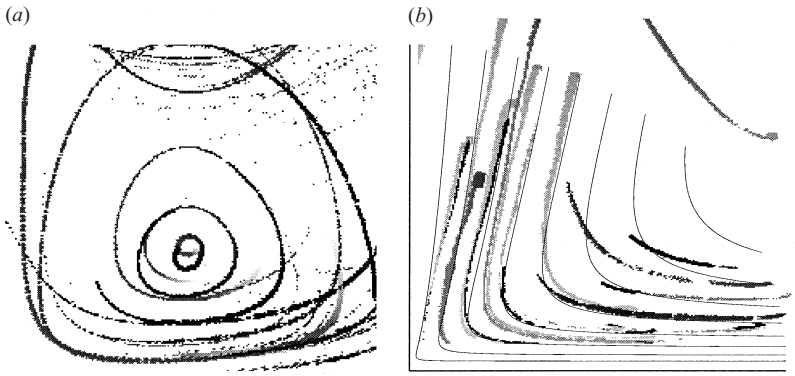

FIGURE 8. Particle tracks constructed from the movement of small air bubbles: (*a*) viewed in a direction perpendicular to the fixed blade; (*b*) viewed in a direction parallel to the line of intersection of the plates; the theoretical Taylor streamlines ψ = constant are superposed as solid curves for comparison.

the particle paths are indeed very nearly closed, and symmetric about the plane $z = 0$. Figure 7(*c*) in which the dye track is viewed nearly along the line of intersection of the planes, provides a visualization of a portion of the Taylor curve; while figure 7(*d*) shows several neighbouring particle paths originating from different points.

The second visualization technique used very small air bubbles illuminated by a strong light source. These bubbles, whose natural rise time was of the order of days, could be regarded as neutrally buoyant 'particles'. Their paths were constructed from a video of the flow using the computer flow-analysis package DIGImage (Dalziel 1992). Figure 8(*a*, *b*) shows resulting particle tracks; (*a*), viewed normal to the fixed blade, shows the (nearly) closed paths, and (*b*), viewed parallel to the contact line, shows what may be described as the 'Taylor projections' $\psi(r, \theta)$ = constant. The streamlines of the Taylor solution are superposed, and the fit is at least qualitatively reasonable.

Finally, reversibility of the flow was tested in the qualitative manner demonstrated by G. I. Taylor in his well-known film 'Low Reynolds Number Hydrodynamics' (Taylor 1966): a blob of dyed fluid was injected, and the lower plate turned slowly through three complete revolutions till the dye appeared well mixed. When the plate was turned in the reverse direction again through three revolutions, the blob of dye reconstituted itself in the original position with just a slight fuzziness due to molecular diffusion. It is perhaps worth remarking that this behaviour is associated with the highly regular closed-streamline character of the flow, as well as with its formal reversibility; in general, three-dimensional steady flows have streamlines that exhibit chaotic wandering (see, for example, Bajer & Moffatt 1990), and will spread a convected dye in an irreversible manner even if they have the formal 'Stokes' property of reversibility.

5. Displacement of centre of rotation

In the experiment described above, an obvious error may arise from any small offset of the vertical blade from the centre of rotation of the lower plate and it is desirable to analyse the effect of such an offset. If this centre of rotation is displaced to the point $x = a$, $y = z = 0$ (as shown in figure 9*a*), then the boundary condition

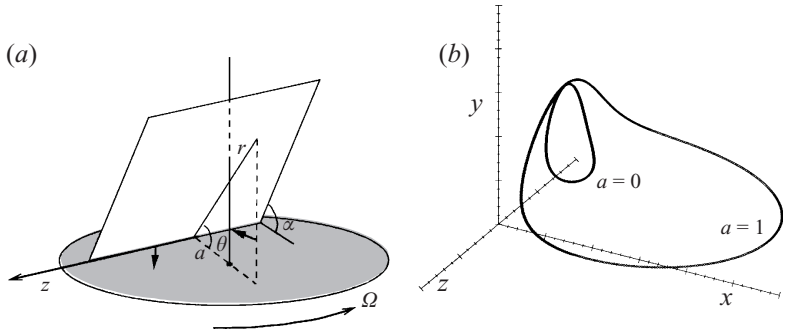

FIGURE 9. (*a*) Geometry with centre of rotation displaced a distance a from the lower plate. (*b*) Closed streamlines for the same initial position for $a = 0$ and for $a = 1$ showing the elongation associated with this displacement.

(2.2*b*) is replaced by

$$\boldsymbol{u} = (\Omega z, 0, -\Omega(r - a)) \quad \text{on } \theta = 0. \tag{5.1}$$

Since the Stokes problem is linear, the new solution is easily found by the addition of a contribution $\hat{w}$ to w satisfying

$$\nabla^2 \hat{w} = 0, \quad \hat{w} = \Omega a \quad \text{on } \theta = 0, \quad \hat{w} = 0 \quad \text{on } \theta = \alpha. \tag{5.2a–c}$$

This contribution is $\hat{w} = \Omega a(1 - \theta/\alpha)$, and the full solution to the Stokes problem becomes

$$u = \Omega z f'(\theta), \quad v = -\Omega z f(\theta), \quad w = -\Omega r f'(\theta) + \Omega a(1 - \theta/\alpha). \tag{5.3a–c}$$

The pressure field (2.5) is unaffected.

The particle paths are now given by

$$\frac{\mathrm{d}r}{z f'(\theta)} = \frac{r\,\mathrm{d}\theta}{-z f(\theta)} = \frac{\mathrm{d}z}{-\Omega r f'(\theta) + a(1 - \theta(\alpha)}. \tag{5.4}$$

The first equality gives $rf(\theta) = \psi_0$ where ψ_0 is constant, as before. Equality of the first and third terms now gives

$$r^2 + z^2 + 2a\psi_0 \int_{\theta_0}^{\theta} \frac{1 - t/\alpha}{(f(t))^2}\,\mathrm{d}t = \text{constant}. \tag{5.5}$$

a closed surface which is a perturbation of a sphere when a is small. The streamlines are still closed curves, the effect of displacing the centre of rotation being to expand and elongate them in the direction of this displacement (figure 9*b*).

6. Differential rotation

A further minor modification of the analysis allows treatment of the situation in which both planes rotate about a common axis but with different angular velocities. Thus, consider the situation in which the blade rotates with angular velocity $\boldsymbol{q} = (0, 0, q)$, and the plane $z = 0$ rotates with angular velocity $(0, 0, \Omega + q)$. If we adopt a frame of reference rotating with angular velocity $\boldsymbol{q}$, then in this frame the blade is fixed, and the boundary conditions are just as before (i.e. (2.2*a*, *b*)). However, the governing equations now include a Coriolis term:

$$(\boldsymbol{u} \cdot \nabla)\boldsymbol{u} + 2\boldsymbol{q} \wedge \boldsymbol{u} = -\nabla \tilde{p} + \nu \nabla^2 \boldsymbol{u}, \qquad \nabla \cdot \boldsymbol{u} = 0, \tag{6.1a, b}$$

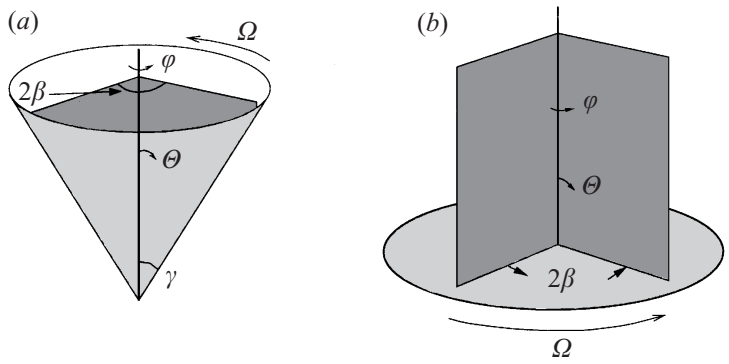

FIGURE 10. (*a*) Two fixed triangular fins $\varphi = \pm\beta$ inside a cone $\Theta = \gamma$ which rotates with angular velocity Ω about the axis $\Theta = 0$. (*b*) The same configuration with $\gamma = \pi/2$.

where $\tilde{p}$ includes, as usual, a contribution from the centrifugal force. Provided $q/\Omega = O(1)$, the Coriolis term $2\boldsymbol{q}\wedge\boldsymbol{u}$ in (6.1*a*) has no effect on the Stokes solution. The inertial correction in the layer where $z = O(r^3\Omega/\nu)$ is however affected. In fact, following the procedure of § 3.2, the change appears in equation (3.15) in which the forcing term on the right-hand side must now include a contribution from the Coriolis term. The modified equation is

$$G'' + 4G = 8f'g + 8q(f''\cos\theta + f'\sin\theta). \tag{6.2}$$

The form of the solution (3.17) for $g_2(\theta)$ is unchanged, but the constants $\{A_i\}$, $\{C_i\}$ in (3.18), (3.19) are replaced by the following values:

$$(\tilde{A}_i) = (A_i) + \tilde{q}\left(-\frac{3\pi}{32}, \frac{1}{8}, -\frac{1}{12}, 0, -\frac{\pi}{24}, 0\right), \tag{6.3}$$

$$(\tilde{C}_i) = (C_i) + \tilde{q}\left(\frac{5\pi}{96}, \frac{\pi^2+4}{96}, \frac{\pi}{24}, \frac{-(\pi^2+6)}{192}\right), \tag{6.4}$$

where $\tilde{q} = (\pi^2 - 4)q/4\Omega$.

7. Flow in a rotating cone with fixed fins

Finally, we consider the geometry indicated in figure 10(*a*), in which a cone of angle γ rotates about its axis which is also the intersection of two rigid triangular 'fins' fixed inside the cone. With spherical polar coordinates (R, Θ, φ) and with basis vectors $\boldsymbol{e}_R, \boldsymbol{e}_\Theta, \boldsymbol{e}_\varphi$, the fins are taken to be $\varphi = \pm\beta$, and the cone is $\Theta = \gamma$. Figure 10(*b*) shows the situation when $\gamma = \pi/2$ so that the cone becomes a rotating plane; the special case in which $2\beta = \pi$ is then the case studied in §§ 2–4 above (when $\alpha = \pi/2$).

We now seek a solution to the Stokes equations (2.1) satisfying the boundary conditions

$$\boldsymbol{u} = 0 \quad \text{on } \varphi = \pm\beta, \qquad \boldsymbol{u} = \Omega R\sin\gamma\,\boldsymbol{e}_\varphi \quad \text{on } \Theta = \gamma. \tag{7.1a,b}$$

We adopt the 'toroidal-poloidal' decomposition of the velocity field

$$\boldsymbol{u} = \nabla\wedge(\boldsymbol{x}T) + \nabla\wedge\nabla\wedge(\boldsymbol{x}P), \tag{7.2}$$

where T and P are scalar fields to be determined. Since the addition to T or P of an arbitrary function of R does not change $\boldsymbol{u}$, we may suppose that T and P have zero

average over any sphere $R =$ constant. Note that the toroidal part of $\boldsymbol{u}$,

$$\nabla \wedge (\boldsymbol{x}T) = -\boldsymbol{x} \wedge \nabla T, \tag{7.3}$$

is a flow whose streamlines lie on spheres $R =$ constant

Substitution of (7.2) in the Stokes equation (2.1a) yields

$$\nu \left[\nabla \wedge \left(\boldsymbol{x}\nabla^2 T\right) + \nabla \wedge \nabla \wedge \left(\boldsymbol{x}\nabla^2 P\right)\right] = \nabla p \tag{7.4}$$

or, taking the curl to eliminate p,

$$-\left(R\nabla_2^2 \nabla^2 T\right)\boldsymbol{e}_R + \nabla_2(\partial(R\nabla^2 T)/\partial R) + (\boldsymbol{e}_R \wedge \nabla_2)(R\nabla^4 P) = 0, \tag{7.5}$$

where $\nabla_2 = \nabla - \boldsymbol{e}_R \partial/\partial R$ is the two-dimensional gradient operator.

Now the boundary conditions (7.1) indicate that, on dimensional grounds,

$$\boldsymbol{u} = \Omega R \hat{\boldsymbol{u}}(\Theta, \varphi), \tag{7.6}$$

where the circumflex indicates a dimensionless function. Here we see the structure of a similarity solution of the first kind (cf. (2.3)). The corresponding scalings of T and P are evidently

$$T = \Omega R \hat{T}(\Theta, \varphi), \qquad P = \Omega R^2 \hat{P}(\Theta, \varphi). \tag{7.7a,b}$$

It follows that $\nabla^2 T$ is proportional to R^{-1} and hence the second term of (7.5) vanishes. The radial component of (7.5) now gives

$$\mathrm{L}^2(\mathrm{L}^2 + 2)\hat{T} = 0, \tag{7.8}$$

where

$$\mathrm{L}^2 = R^2\nabla_2^2 = \frac{1}{\sin\Theta}\left[\frac{\partial}{\partial\Theta}\left(\sin\Theta\frac{\partial}{\partial\Theta}\right) + \frac{1}{\sin\Theta}\frac{\partial^2}{\partial\varphi^2}\right]. \tag{7.9}$$

The non-radial components of (7.5) give $\nabla^4 P = 0$ (using the zero-average property mentioned above) and, using (7.7), this reduces to

$$\mathrm{L}^2(\mathrm{L}^2 + 6)\hat{P} = 0. \tag{7.10}$$

Equations (7.8), (7.10) have to be solved subject to the boundary conditions (7.1), i.e.

$$\hat{\boldsymbol{u}} = 0 \quad \text{on } \varphi = \pm\beta, \qquad \hat{\boldsymbol{u}} = \sin\gamma \boldsymbol{e}_\varphi \quad \text{on } \Theta = \gamma. \tag{7.11a,b}$$

We already know the solution in the special case when $2\beta = \pi$, $\gamma = \pi/2$; in this case, taking due account of the change of coordinate system,

$$\hat{T} = (r/R)f(\theta), \quad \hat{P} = 0, \tag{7.12a,b}$$

where $f(\theta)$ is still given by (2.13a). We conjecture that $\hat{P} = 0$ in the general case also (i.e. that the required flow is purely toroidal, with streamlines on spheres $R =$ constant). Under this assumption, the problem that remains to be solved is (7.8) with boundary conditions (from 7.11)

$$\partial\hat{T}/\partial\varphi = \hat{T} = 0 \quad \text{on } \varphi = \pm\beta, \tag{7.13a}$$

$$\hat{T} = 0, \quad \partial\hat{T}/\partial\Theta = \sin\gamma \quad \text{on } \Theta = \gamma. \tag{7.13b}$$

Also, since $\boldsymbol{u} \to 0$ as $\Theta \to 0$, $\hat{T}$ must be $o(\Theta)$ as $\Theta \to 0$.

We limit consideration here to the behaviour of the solution to this problem near to the 2β-corner where $\Theta \ll 1$. In this region, (7.8) degenerates to

$$\mathrm{L}_1^4\hat{T} = 0 \quad \text{where} \quad \mathrm{L}_1^2 = \frac{1}{\Theta}\frac{\partial}{\partial\Theta}\Theta\frac{\partial}{\partial\Theta} + \frac{1}{\Theta^2}\frac{\partial^2}{\partial\varphi^2}. \tag{7.14a,b}$$

The equation (7.14*a*), being homogeneous in Θ, admits solutions of the form

$$\hat{T} = \Theta^{\lambda} f_{\lambda}(\varphi), \tag{7.15}$$

where λ must be determined through satisfying the boundary conditions (7.13*a*). The analysis now exactly parallels that of Moffatt (1964) and the conclusions likewise: for $2\beta < 146^{\circ}$, a sequence of eddies is present as $\Theta \to 0$. The streamlines of these eddies lie on spheres $R =$ constant, and for varying R, they scale linearly in R, and so form cones of eddying motion in alternating directions. This asymptotic behaviour is that of a similarity solution of the second kind (Barenblatt 1996) which is evidently contained within the similarity solution (7.6) of the first kind. As far as we are aware, this is the first time that this sort of double similarity structure has been identified in a steady flow.

REFERENCES

Bajer, K. & Moffatt, H. K. 1990 On a class of steady confined Stokes flows with chaotic streamlines. *J. Fluid Mech.* **212**, 337–363.

Barenblatt, G. I. 1996 *Scaling, Self-Similarity, and Intermediate Asymptotics*. Cambridge University Press.

Batchelor, G. K. 1967 *An Introduction to Fluid Dynamics*. Cambridge University Press.

Dalziel, S. B. 1992 DIGImage: *System Overview*. Cambridge Environmental Research Consultants Ltd.

Hancock, C., Lewis, E. & Moffatt, H. K. 1981 Effects of inertia in forced corner flows. *J. Fluid Mech.* **112**, 315–327.

Moffatt, H. K. 1964 Viscous and resistive eddies near a sharp corner. *J. Fluid Mech.* **18**, 1–18.

Moffatt, H. K. 1979 The asymptotic behaviour of solutions of the Navier–Stokes equations near sharp corners. In *Approximate Methods for Navier–Stokes Problems*. Lecture Notes in Mathematics, vol. 771 (ed. R. Rautmann), pp. 371–380. Springer.

Moffatt, H. K. & Duffy, B. R. 1980 Local similarity solutions and their limitations. *J. Fluid Mech.* **96**, 299–313.

Moffatt, H. K. & Mak, V. 1999 Corner singularities in three-dimensional Stokes flow. In *Nonlinear Singularities in Deformation and Flow* (ed. D. Durban & J. R. A. Pearson), pp. 21–26. Kluwer.

Takahashi, K., Sasaki, M., Arai, K. & Saito, S. 1982 Effects of geometrical variables of helical ribbon impellers on mixing of highly viscous Newtonian liquids. *J. Chem. Engng Japan* **15**, No. 3, 217–224.

Tatterson, G. B., Brodkey, R. S. & Calabrese, R. V. 1991 Move mixing technology into the 21st century. *Chem. Engng Prog.* **87**, 45–48.

Taylor, G. I. 1960 Similarity solutions of hydrodynamic problems. In *Aeronautics and Astronautics* (*Durand Anniv. Vol.*), pp. 21–28. Pergamon.

Taylor, G. I. 1962 On scraping viscous fluid from a plane surface. Reprinted in *The Scientific Papers of Sir Geoffrey Ingram Taylor*, vol. IV (ed. G. K. Batchelor), pp. 410–413. Cambridge University Press.

Taylor, G. I. 1966 *Low Reynolds Number Hydrodynamics*. 16 mm film, 32 mins, colour, sound. Educational Services Ltd., Newton Mass.

Weast, R. C. 1971 *CRC Handbook of Chemistry and Physics*, 52nd Edn. Chemical Rubber Co.